Microstructure evolution of an Al-Pd-Co alloy

Ľ. Kahalová[1], M. Kusý[1], J. Buršík[2], M. Svoboda[2], E. Illeková[3], P. Švec[3], J. Dolinšek[4], J. Janovec[1]*

[1]*Faculty of Materials Science and Technology, Slovak University of Technology, Bottova 23, 917 24 Trnava, Slovak Republic*
[2]*Institute of Physics of Materials, Academy of Sciences of the Czech Republic, Žižkova 22, 616 62 Brno, Czech Republic*
[3]*Institute of Physics, Slovak Academy of Sciences, Dúbravská cesta 9, 845 11 Bratislava, Slovak Republic*
[4]*Institute of Jožef Stefan, University of Ljubljana, Jamova 39, 1000 Ljubljana, Slovenia*

Received 11 March 2008, received in revised form 8 July 2008, accepted 15 July 2008

Abstract

A complex metallic alloy of the nominal chemical composition of 73.5Al-11Pd-15.5Co (at.%) was annealed at 1000 °C for 92 hours and then investigated with light microscopy, differential thermal analysis, scanning electron microscopy including energy and wavelength dispersive X-ray spectroscopy, and X-ray diffraction. The annealed samples (as-received state) and the samples after the thermal cycling in DTA were found to consist of the same microstructural constituents corresponding to the ternary U-phase, binary δ-phase, and a non-identified phase. The U-phase showed the compositional stability in a broad temperature range. The stabilization of the δ-phase during cooling was found to be accompanied with the decrease of cobalt content.

K e y w o r d s: complex metallic alloys, Al-Pd-Co system, differential thermal analysis, U-phase, δ-phase

1. Introduction

Complex metallic alloys (CMAs) are members of a huge group of largely unknown multicomponent alloys. In these alloys, phases are formed with crystal structure based on giant unit cells containing many tens, up to more than thousand atoms per unit cell [1–3]. Inside the cells the atoms are arranged in clusters with a multitude of different coordination polyhedra where icosahedral coordination environments play a prominent role [4]. As a consequence, the structures of CMAs show the duality. On the scale of several nanometers, CMAs are periodic crystals, whereas on the atomic scale they resemble quasicrystals. The clusters are distributed quasiperiodically in the quasicrystals, while they are arranged periodically in the CMAs [5–7]. The atom arrangement strongly influences the electronic structure and lattice dynamics what leads to unique combinations of properties. For instance, the good metallic electric conductivity is combined with the low thermal conductivity, the good light absorption is combined with the high temperature stability, or the high metallic hardness is combined with the wetting by liquids [1, 7].

The investigation of new combinations of properties has been often connected with searching for new quasicrystal forming systems. Therefore, many different metal alloys based on copper, gallium, magnesium, aluminium, nickel, tantalum, titanium, zinc, zirconium, cadmium, hafnium etc. have been investigated [8, 9]. The binary Al-TM (TM – transitional metal) systems containing 60–85 at.% of aluminium and the ternary Al-TM-TM systems have been investigated mostly [10]. These extensive studies have demonstrated a need for the reconsideration of binaries and ternaries of the concerned systems.

Recently, few studies only have been focused on the Al-Pd-Co system and the phases identified are listed in Tables 1 and 2. To extend the knowledge about this system, an Al-Pd-Co alloy was investigated in the present work. The attention was paid to the characterization of the alloy microstructure and microchemical

*Corresponding author: tel.: +421 918 64 60 72; fax: +421 33 552 10 07; e-mail address: jozef.janovec@stuba.sk

Table 1. Binary phases observed in the Al-Pd-Co system [11]

Phase	Al (at.%)	Maximal solubility (at.%) of the third element at 790 °C	Space group or symmetry	Lattice parameters			
				a (nm)	b (nm)	c (nm)	β (°)
Al-Co alloy system							
Al_9Co_2	81.9	2.6	$P2_1/a$	0.85565	0.6290	0.62130	94.76
O-$Al_{13}Co_4$	76.5	< 0.3	$Pmn2_1$ or Pnmn	0.8158	1.2347	1.4452	–
M-$Al_{13}Co_4$	75.8	2.7	C2/m	1.5173	0.81090	1.2349	107.84
Z	74.5	1.6	C-centr. Monocl.	3.984	0.8148	3.223	107.97
Al_5Co_2	71.4	3.0	$P6_3/mmc$	0.76717	–	0.76052	–
AlCo(β)	~ 21.5–52		$Pm\bar{3}m$	0.2854	–	–	–
Al-Pd alloy system							
ε_6	73.1–74.6	15.3	$Pna2_1$	2.35	1.68	1.23	–
ε_6^*	As ε_6		Orthorhomb.	(4.70)	3.36	2.46	–
ε_{28}	71.9		C2mm	2.35	1.68	5.70	–
$Al_3Pd_2(\delta)$	?–61.1	4.0	$P\bar{3}m1$	0.4227	–	0.5167	–
AlPd(β)	?–56.5	19.8	$Pm\bar{3}m$	0.3036	–	–	–

Table 2. Ternary phases observed in Al-Pd-Co system [11]

Phase	Space group or crystal symmetry	Lattice parameters				At. composition (at.%)		
		a (nm)	b (nm)	c (nm)	β (°)	Al	Pd	Co
W	$Pmn2_1$	2.36	0.82	2.07	–	72.0	4.8	23.2
V	P121, P1m1 or P12/m1	1.0068	0.3755	0.6512	102.38	70.0	10.0	20.0
U	P121, C1m1 or C12/m1	1.9024	2.90	1.3140	117.26	69.1	16.5	14.4
F	$P2_1/a\bar{3}$	2.4397	–	–	–	72.8	9.0	18.2
C_2	$Fm\bar{3}$	1.5507	–	–	–	63.0	26.5	10.5
Y_2	Immm	1.5451	1.2105	0.7590	–	75.5	3.8	20.7
ε_{22}	orthorhombic	2.35	1.68	5.70	–	72.0	20.0	8.0
ε_{34}	orthorhombic	2.35	1.68	7.01	–	70.0	15.0	15.0

homogeneity. The occurrence, distribution and stability of binary and ternary phases were also determined.

2. Experimental

The alloy with the nominal chemical composition of 73.5Al-11Pd-15.5Co (at.%) was prepared by melting the pure constituents under helium atmosphere in an induction furnace. The as-cast ingots were then crushed into the powder of the granulometric fraction between 20 and 50 μm. The powder was compacted in a graphite cell, sintered at higher temperature using a uniaxial pressure of 15 MPa and annealed at 1000 °C for 92 hours.

The structure and properties of the sintered and annealed bulk material (called as-received in this work) were studied with light microscopy, scanning electron microscopy (SEM), high-temperature differential thermal analysis (DTA), and X-ray diffraction (XRD). In the investigations, a scanning electron microscope Jeol JMS-6460 with tungsten cathode, acceleration voltage of 20 kV, and detectors for secondary (SEI) and backscattered (BSE) electrons as well as an X-ray diffractometer Philips PW 1710 with acceleration voltage of 40 kV and Co Kα1 radiation were used. Samples for light microscopy were polished and then etched with 2 % Keller. Microhardness measurements under loading of 10 g ($HV_{0.01}$) were also performed. The microstructural constituents on polished and unetched samples were characterized with SEM using the energy dispersive X-ray spectroscopy (EDS) and the wavelength dispersive X-ray spectroscopy (WDS). These methods were also used for the determination of the real chemical composition. The composition of the as-received sample was found to be 69.5Al-17.2Pd-13.3Co (±0.3 at.%). DTA was performed in dynamic argon atmosphere with the heating (cooling) rate of 10 °C min^{-1} up to 1334 °C.

3. Results

3.1. Light microscopy and microhardness

Light micrographs of the studied material are

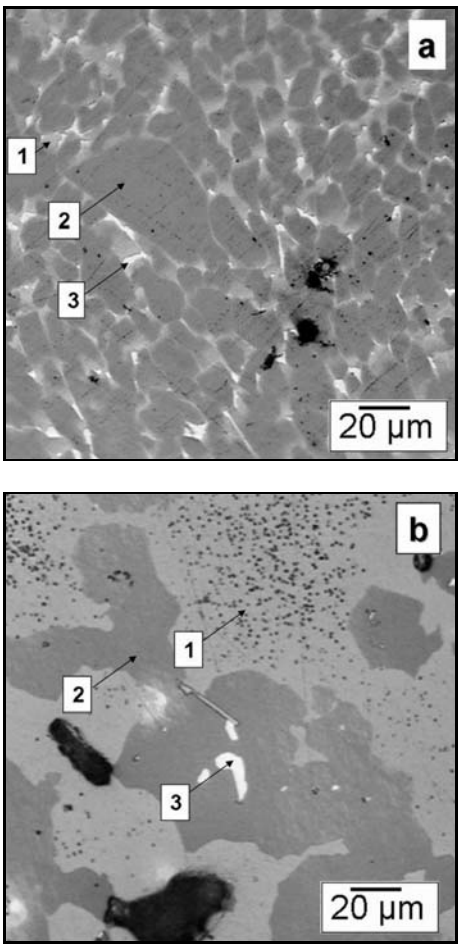

Fig. 1. Light micrographs of (a) as-received state, (b) state after DTA. The grey, charcoal and white areas are marked by symbols 1, 2 and 3, respectively.

shown in Fig. 1. As it is clear from Fig. 1a, the microstructure of the alloy in the as-received state consists of more areas exhibiting different colours. The charcoal areas (marked with 2) dominating in the microstructure form discrete grains of various sizes and shapes. The white mainly longitudinal areas (marked with 3) are randomly distributed in the whole volume. The volume portion of white areas is evidently lower than that of the charcoal areas (Table 3). The grey areas (marked with 1) form continuous network around the discrete charcoal and white grains. The microstructure of the alloy after the DTA experiments (Fig. 1b) contains identical areas as documented for the as-received state. However, it does not form grains any more. In the all samples studied pores (black localities) were identified. The pores are present in a higher extent in the sample after the DTA experiments. In the polarized light, the observed samples did not show any birefringent behaviour.

The values of microhardness are given in Table 3 for the particular areas. The grey areas in the as--received state show diffuse boundaries with the charcoal areas that precluded the reproducible measurement of their microhardness. The microhardness values of the grey area are therefore given for the state after DTA only (Table 3). With respect to a small size of the white grains, low loads (10 g) were used in the measurements. As a consequence, very small (about 3 μm in diagonal) hardly measurable indentations were obtained. Volume portions of particular phases (Table 3) were determined using an image analyser IMPOR PRO 32. No standard deviations are given in Table 3 for volume portions, because of small differences between the measured values.

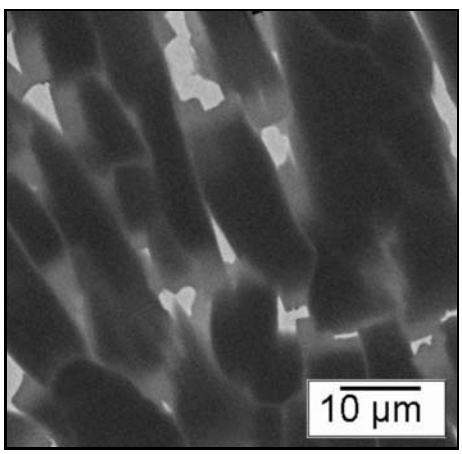

Fig. 2. Backscattered electron micrograph of as-received state.

Table 3. Volume portions and microhardness ($HV_{0.01}$) of areas present in the microstructure

Area	As-received state		State after DTA experiments	
	Volume portion in %	$HV_{0.01}$	Volume portion in %	$HV_{0.01}$
Pores	1.8		8.1	
White	2.4	720 ± 22	1.4	727 ± 14
Charcoal	84.4	429 ± 16	43.2	435 ± 28
Grey	11.4	–	47.3	507 ± 33

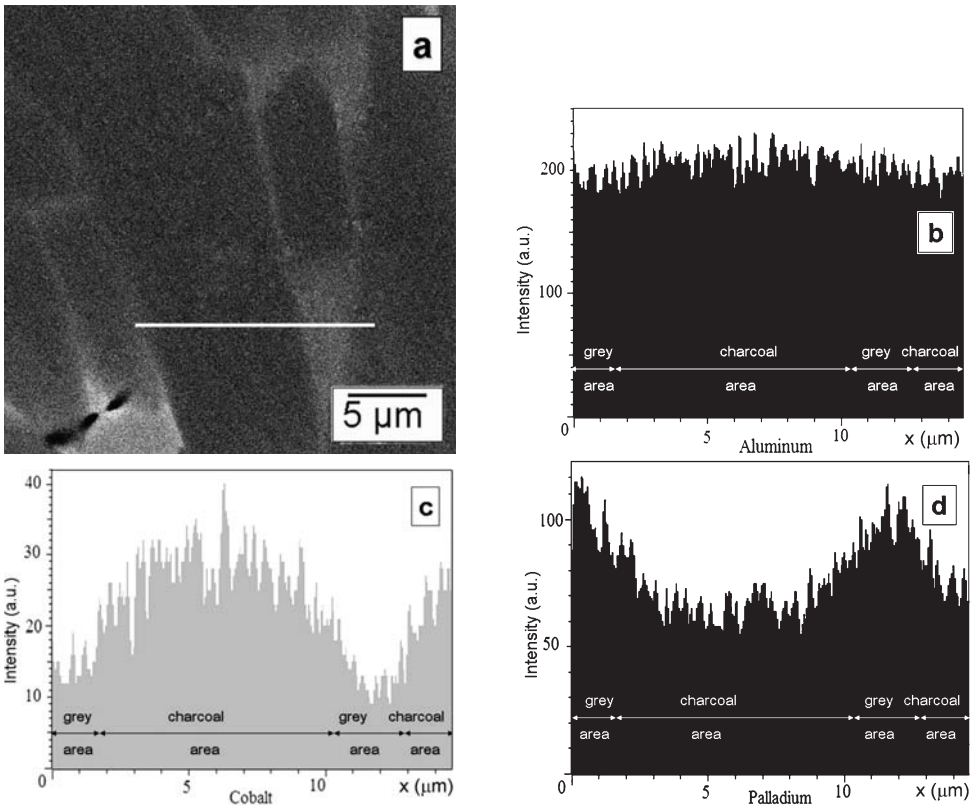

Fig. 3. Distribution of aluminium (b), cobalt (c), and palladium (d) along the abscissa shown in the microstructure of the as-received state (a), EDS/SEM.

Table 4. Measured chemical compositions of observed areas compared with literature data published for Al-Pd-Co system

Phase	Measured chemical composition (at.%)				Chemical composition according to [11] (at.%)			Supposed phase
	Method	Al	Pd	Co	Al	Pd	Co	
Charcoal	WDS	70.51 ± 0.04	15.15 ± 0.15	14.34 ± 0.11	69.1	16.5	14.4	U
	EDS	70.21 ± 0.08	19.46 ± 0.73	10.34 ± 0.81				
White	WDS	59.52 ± 1.27	39.05 ± 0.98	1.43 ± 0.28	≤ 61.1	≥ 34.9	up to 4	Al_3Pd_2 (δ)
	EDS	56.48 ± 0.11	42.32 ± 0.14	1.22 ± 0.04				
Grey	WDS	69.84 ± 0.41	20.76 ± 4.43	9.40 ± 4.02				
	EDS	68.44 ± 1.43	23.90 ± 0.85	7.68 ± 0.58				

3.2. Scanning electron microscopy

BSE micrograph of the unetched as-received state is shown in Fig. 2. Various areas present in the alloy microstructure exhibit different chemical compositions. From the imaging principles for the BSE mode it comes out that the white areas are enriched with the heavier palladium and the darker areas contain higher amount of the lighter aluminium. This finding was later supported with compositional measurements comprising the mapping and the line analysis in the EDS mode as well as with the WDS analysis.

The line analysis was performed along the abscissa illustrated in Fig. 3a. In Figs. 3b–d, changes in contents of analysed elements are shown. It follows from the comparison of the diagrams that the amount of cobalt decreases with increasing the palladium amount and vice versa. Aluminium seems to be distributed quite homogeneously. However, the lower concentrations of aluminium were observed in the white-colour area or along the grain boundaries.

For gaining the exact chemical composition of the observed areas, EDS as well as WDS analyses were used. The average concentrations are listed in Table 4, separately for each method and analysed area. Literature data concerning the chemical compositions of

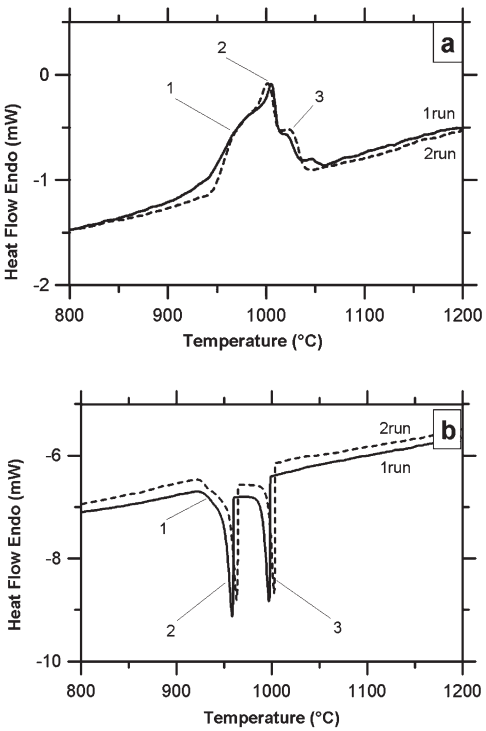

Fig. 4. DTA record of analysed sample: (a) heating curves, (b) cooling curves. Symbols 1, 2 and 3 were used to label peaks corresponding to grey, charcoal and white areas, respectively.

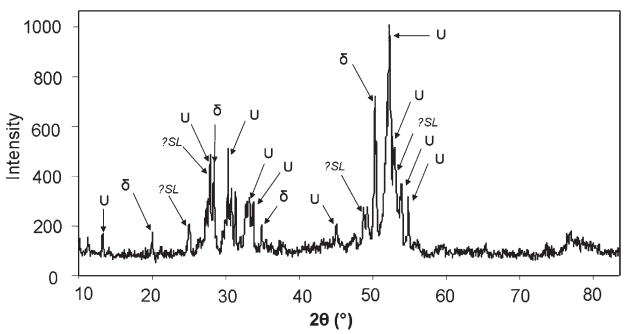

Fig. 5. Diffraction pattern of the alloy in as-received state.

the phases identified in the Al-Pd-Co system are also given in Table 4. By comparison of the measured values with the literature data the phases supposed to be present in the studied alloy were determined.

3.3. Differential thermal analysis

DTA of the as-received state was performed in the temperature range from 20 to 1334 ℃. The experiment consisted of two heating and two cooling runs as shown in Fig. 4a,b. The heating curves exhibit three slightly overlapped peaks for each run, whereas the cooling curves contain two peaks with sharp onsets and in the second run a hint of the third peak. Small variations in reaction enthalpies for each cooling ($\Delta H = 305\,\mathrm{J\,g^{-1}}$ in the first run and $316\,\mathrm{J\,g^{-1}}$ in the second run, always $\pm 2\,\mathrm{J\,g^{-1}}$) and heating ($\Delta H = 323\,\mathrm{J\,g^{-1}}$ in the first run and $317\,\mathrm{J\,g^{-1}}$ in the second run) runs were observed. The enthalpy of the first melting is higher than that of the second melting; however it characterizes the as-received sample, a state slightly different from the DTA heat-treated one. Differences between the reaction enthalpies corresponding to the heating and cooling regimes of the same run do not exceed $12\,\mathrm{J\,g^{-1}}$ (approximately 4 %).

3.4. X-ray diffraction

XRD was performed to discover phases present in the as-received state. As it is shown in Fig. 5, the diffraction record is very complex (tens of peaks are captured in it). To evaluate the pattern, the Powder Diffraction File and the diffraction data published by Shaobo Mi et al. [12] were used. The ternary U-phase and the binary Al_3Pd_2 (δ-phase) were identified in the alloy. Besides peaks corresponding to these phases, some others of lower intensities (marked as *SL-solidified liquid*) were observed in the spectrum (Fig. 5). According to the peak heights, the U-phase was found to be a dominant one. The remaining non-indexed peaks belong either to the third phase or to the mixture of other minor phases. Measured values of 2θ together with Miller's indices h, k, l and corresponding phases are listed in Table 5.

4. Discussion

The investigated alloy was prepared with the intention to obtain homogeneous ε-phase. Unfortunately, the chemical composition of the alloy was changed during the preparation and subsequent annealing in term of increased palladium, and decreased aluminium and cobalt contents. The alloy consists at least of three areas differing from each other in colour as it is shown in Fig. 1a. The position of the alloy in the ternary Al-Pd-Co diagram for 1000 ℃ published by Yurechko et al. [11] is illustrated in Fig. 6. The solid and empty circles represent nominal and real chemical compositions of the alloy, respectively. The dashed curves point out chemical compositions of constituents corresponding to grey (1), charcoal (2) and white (3) areas characterized by light microscopy and WDS (EDS) analysis. The major charcoal area was found to contain about 15 at.% of both palladium and cobalt next to aluminium (Tables 3, 4). It is situated close to the single U-phase region in the ternary diagram (Fig. 6). The minor white area is palladium-rich and contains traces of cobalt. In the ternary dia-

Table 5. XRD data corresponding to Fig. 5

2 theta$_{measured}$ (°)	I/I_0	h	k	l	Phase
13.2928	10.12	–2	2	1	U
25.0625	11.59				*?SL*
27.4161	24.87				*?SL*
27.9002	45.49	1	7	1	U
28.4021	33.97	1	0	0	δ
30.2975	48.53	–4	4	3	U
30.794	30.53	–2	8	1	U
31.3502	28.71	–3	7	2	U
32.7678	20.52	1	9	0	U
33.2032	25.04	–1	9	1	U
33.7303	23.78	0	8	2	U
34.9117	13.79	0 1	1 0	1 1	δ
45.0755	11.9	–5	5	5	U
48.7683	21.27				*?SL*
49.2238	22.19	6	2	2	U
50.3412	47.73	0 1	1 0	2 2	δ
51.9	66.32	0	14	1	U
52.276	100	–7	9	1	U
52.8154	51.79	–6	8	5	U
53.113	39.99				*?SL*
53.9163	33.02	–8	8	3	U
54.8543	25.79	–8	6	5	U
76.4576	9.99				*?SL*
76.8717	9.59				*?SL*

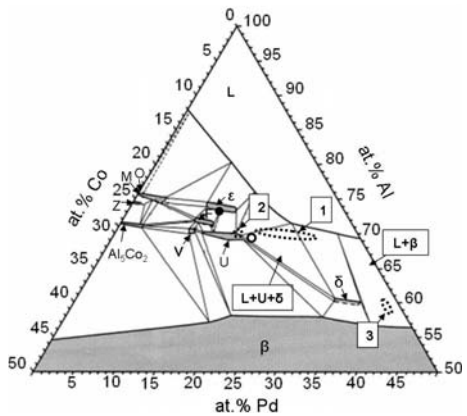

Fig. 6. Partially modified ternary diagram for Al-Pd-Co system at 1000 °C [11].

gram it falls into the liquid + β region. The grey--area forming network along the charcoal areas shows enhanced palladium and reduced cobalt contents related to the nominal alloy composition. This constituent corresponds to the elliptic object situated in the three-phase liquid + U + δ region of the ternary diagram at 1000 °C. It is positioned close to the single--phase liquid area.

As follows from the results obtained by light microscopy (Fig. 1a), EDS (Fig. 3), DTA (Fig. 4), and XRD (Fig. 5), the charcoal area (marked also 2 in this work) corresponds to the U-phase and the white area (marked also 3) is the binary Al_3Pd_2 (δ-phase) alloyed with cobalt. The DTA curves indicate the presence of liquid phase in the alloy at temperatures about 1000 °C. This is also in accordance with the isothermal section of ternary diagram for 1000 °C presented by Yurechko et al. [11], Fig. 6. The phase represented by the grey area is marked with symbols 1 in Fig. 1a and *SL* in Fig. 5 and Table 5. It corresponds to the phase, which is liquid at 1000 °C and co-exists with the two identified solid phases. During the cooling from the annealing temperature, the liquid phase solidified and a new crystalline phase(s) were formed (see peaks marked as *SL* in Fig. 5). Unfortunately, any available structure did not show any accordance with the *SL* peaks in the XRD spectrum. Thus, the structure of this constituent was not determined. The decomposition and/or the formation of crystalline objects in the *SL* constituent are associated with the appearance of one peak only (it is marked with 1 in the DTA curves in Fig. 4). This shows the single-phase character of the *SL* constituent.

The U-phase did not undergo any significant changes related to its structure and/or composition during the cooling from the annealing temperature. The charcoal area (Fig. 1) analysed at room temperature exhibited the similar chemical composition as predicted for the U-phase at 1000 °C (see position of area 2 related to the single-phase U-region in Fig. 6). This is in accordance with the findings published by Yurechko et al. [11]. Completely different behaviour as described for the ternary U-phase shows the binary δ-phase. The single-phase δ region is shifted to the aluminium axis in the ternary diagram when the temperature decreases [11]. It means that the cobalt content in the δ-phase decreases with decreasing temperature in term of the stabilization of this binary phase. It is therefore acceptable that the δ-phase overcomes compositional changes during the cooling without any structural transformations. Thus, the δ-phase analysed at room temperature shows chemical composition falling into the two-phase liquid + β region in the ternary diagram proposed for 1000 °C. This is due to the reduction of cobalt content in the δ-phase during the cooling.

The sample after DTA consists of the same microstructural constituents (phases) showing the same colours (compare Figs. 1a,b) and similar microhardness values (Table 3) as the sample of the as-received state. Thus, the sample after DTA contains the U-phase (marked with symbol 2 in Figs. 1 and 6), the δ-phase (3) and solidified liquid (1) as it was identified for the as-received state. The volume portion of pores increased in the sample after DTA (Table 3, Fig. 1). This is contradictory to the expectation, because the

sample was totally re-melted at the maximum temperature of thermal cycles (1334 ℃) as follows from the DTA records (Fig. 4). The reason for the increase of pores after DTA should be the effect of dynamic argon, which forms bubbles penetrating the melt. The volume portions of U- (2) and δ- (3) phases decreased and the volume portion of the solidified liquid increased after thermal cycling if compared to the as-received state (Table 3, Fig. 1). It is acceptable, because the holding time at 1000 ℃ of the DTA tested sample was about 6 seconds and the total cooling time took about 2 h. For comparison, the annealing time of the as-received sample at 1000 ℃ was 92 h. It can be expected that the conditions at DTA did not allow the growth of the U- and δ-phases from liquid in near equilibrium amount. As a result, the volume portion of the *SL* constituent (47.3 %) is significantly higher than it was determined for the as-received state (Table 3).

5. Conclusions

Two states of the complex metallic alloy with the nominal chemical composition of 73.5Al-11Pd-15.5Co (at.%) have been investigated: the original as-received state (after annealing at 1000 ℃ for 92 hours) and the state after the DTA experiments. The results obtained with various experimental techniques can be summarized as follows:

1. Both investigated samples were found to consist of the same microstructural constituents corresponding to the ternary U-phase, binary δ-phase and a non-identified phase. In the microstructures, small amount of pores was observed.

2. The U-phase showed the compositional stability in a huge temperature range. The stabilization of the δ-phase (Al_3Pd_2 alloyed with cobalt) during cooling from the annealing temperature was associated with a decrease in the cobalt content.

3. It was found out that the volume fractions of the particular phases and pores were changed during thermal cycling. After the DTA, the volume portions of U- and δ-phases in the microstructure decreased opposite to the non-identified phase and pores.

Acknowledgements

The authors wish to thank the Grant Agency of the Ministry of Education of the Slovak Republic and the Slovak Academy of Sciences for financial support under the contract No. 1/4107/07 as well as the Czech Science Foundation for financial support under the contract No. 106/07/1259.

References

[1] http://www.temas.ch/WWWTEMAS/TEMAS_Homepage.nsf/vwRes/CMA1/$FILE/PROSPECT_CMA.pdf
[2] CHWALEK, L. M.—BALANETSKYY, S.—THOMAS, C.—ROITSCH, S.—FEUERBACHER, M.: Intermetallics, *15*, 2007, p. 1678.
[3] HEGGEN, M.—DENG, D.—FEUERBACHER, M.: Intermetallics, *15*, 2007, p. 1425.
[4] URBAN, K.—FEUERBACHER, M.: Journal of Non-Crystalline Solids, *334&335*, 2004, p. 143.
[5] SMONTARA, A.—SMILJANIĆ, I.—BILUŠIĆ, A.—GRUSHKO, B.—BALANETSKYY, S.—JAGLIČIĆ, Z.—VRTNIK, S.—DOLINŠEK, J.: Journal of Alloys and Compounds, *450*, 2008, p. 92.
[6] DOLINŠEK, J.—APIH, T.—JEGLIČ, P.—SMILJANIĆ, I.—BILUŠIĆ, A.—BIHAR, Ž.—SMONTARA, A.—JAGLIČIĆ, Z.—HEGGEN, M.—FEUERBACHER, M.: Intermetallics, *15*, 2007, p. 1367.
[7] SMONTARA, A.—SMILJANIĆ, I.—BILUŠIĆ, A.—JAGLIČIĆ, Z.—KLANJŠEK, M.—ROITSCH, S.—DOLINŠEK, J.—FEUERBACHER, M.: Journal of Alloys and Compounds, *430*, 2007, p. 29.
[8] HUTTUNEN-SAARIVIRTA, E.: Journal of Alloys and Compounds, *363*, 2004, p. 150.
[9] JEEVAN, S. H.—RANGANATHAN, S.: Journal of Non-Crystalline Solids, *334&335*, 2004, p. 184.
[10] GRUSHKO, B.—VELIKANOVA, YA. T.: Journal of Alloys and Compounds, *367*, 2004, p. 58.
[11] YURECHKO, M.—GRUSHKO, B.—VELIKANOVA, YA. T.—URBAN, K.: Journal of Alloys and Compounds, *337*, 2002, p. 172.
[12] SHAOBO, M.—YURECHKO, M.—JINSONG, WU.—GRUSHKO, B.: Journal of Alloys and Compounds, *329*, 2001, p. L1.